Hydrol. Earth Syst. Sci. Discuss., 10, 8503–8536, 2013
www.hydrol-earth-syst-sci-discuss.net/10/8503/2013/
doi:10.5194/hessd-10-8503-2013


Hydrology and Earth System Sciences
Discussions
Open Access







# Impacts of climate and forest changes on streamflow and water balance in a mountainous headwater stream in Southern Alberta

**V. Mahat**[1] **and A. Anderson**[1,2]

[1]Department of Renewable Resources, University of Alberta, 211 Human Ecology Building, Edmonton, AB T6G 2H1, Canada
[2]Water Program Lead, Foothills Research Institute, P.O. Box 6330, Hinton, AB T7V 1X6, Canada

Received: 14 June 2013 – Accepted: 21 June 2013 – Published: 2 July 2013

Correspondence to: V. Mahat (mahat@rams.colostate.edu) and
A. Anderson (aanderson@foothillsri.ca)

Published by Copernicus Publications on behalf of the European Geosciences Union.

## Abstract

Rivers in Southern Alberta are vulnerable to climate change because much of the river water originates as snow in the eastern slopes of the Rocky Mountains. Changes in likelihood of forest disturbance (wildfire, insects, logging, etc.) may also have impacts that are compounded by climate change. This study evaluates the impacts of climate and forest changes on streamflow in the upper parts of the Oldman River in Southern Alberta using a conceptual hydrological model, HBV-EC in combination with a stochastic weather generator (LARS-WG) driven by GCM (Global Climate Model) output climate data. Three climate change scenarios (A1B, A2 and B1) are selected to cover the range of possible future climate conditions (2020s, 2050s, and 2080s). GCM projected less than a 10 % increase in precipitation in winter and a similar amount of precipitation decrease in summer. These changes in projected precipitation resulted in up to a 200 % (9.3 mm) increase in winter streamflow in February and up to a 63 % (31.2 mm) decrease in summer flow in June. This amplification is mostly driven by the projected increase in temperature that is predicted to melt winter snow earlier, possibly resulting in lower water availability in the snowmelt dominated regions during the summer. Uncertainty analysis was completed using a guided GLUE (generalized likelihood uncertainty estimation) approach to obtain the best 100 parameter sets and associated ranges of streamflows. The impacts of uncertainty were higher in spring and summer flows than in winter and fall flows. Forest change compounded the climate change impact by increasing winter flow; however, it did not reduce the summer flow.

## 1 Introduction

The eastern slopes of the Rocky Mountains in Alberta, Canada have the highest regional precipitation and runoff ratios (annual streamflow as a proportion of annual precipitation). This generates the majority of streamflow for many rivers including the Oldman River which provides water for domestic and recreational purposes and supports a broad base of regional agriculture and fisheries industries in Southern Alberta (Bladon et al., 2008; Emelko et al., 2011; Silins et al., 2009; Stone et al., 2001). Hydrology of mountainous regions are most likely to be affected by climate change as precipitation would change from snow to rain in a warming climate (IPCC, 2007). Headwater streams and rivers supporting the Oldman River system originates as snow in the eastern slopes of the Rocky Mountain and are vulnerable to a warming climate. Forest change may compound the impacts of climate change. Given the present near full allocation of water for human use in this region, along with the possibility of longer-term limitations in water supply, understanding and predicting how climate and forest changes in this region are likely to affect the production/timing of streamflow are increasingly important (Silins et al., 2009).

There have been a number of studies that have delved into the potential effects of climate change on hydrology and water resources in many regions. Apparent trends in streamflow due to climate change are both increasing and decreasing (Arnell, 1999; Zheng et al., 2009). Arnell (1999) investigated the climate change impacts on water supply on the global scale and reported up to a 15 % decrease in streamflow in major river basins by the year 2050. Studies carried out in different regions of North America, i.e. Jha et al. (2004) (Upper Mississippi River Basin, USA), Stone et al. (2001) (Missouri River Basin, USA), Hamlet and Lettenmaier (1999) (Columbia River Basin, USA), Kienzle et al. (2012) (North Saskatchewan River basin, AB, Canada) and Stahl et al. (2008) (Bridge River basin, BC, Canada] have reported a streamflow increase of up to 80 % in fall and winter and a 10 to 20 % decrease in summer. Barnett et al. (2005) studied a number of large basins around the globe and reported streamflow regime in snowmelt-dominated river basins is the most sensitive. As melting of winter snow occurs earlier in spring due to temperature rise, there is likely to be future water scarcity in the snow melt dominated regions during the summer. Other studies (e.g. Barnett et al., 2008; Hidalgo et al., 2009; Mote, 2003; Pierce et al., 2008) that are focused on the snowmelt dominated regions have also reported a reduction in snow and an early shift in the timing of the streamflow.





HESSD
10, 8503–8536, 2013

GCMs (General Circulation Models or Global Climate Models) are widely used to project future climates under assumed greenhouse gas emission scenarios, both in space and time (e.g. IPCC, 2007; Mehrotra and Sharma, 2010). However, the projections from these models are typically provided at coarse resolutions, i.e. 200 km or more, in space and monthly time periods (Wang et al., 2011). The hydrologic processes of interest normally occur at scales on the order of tens to thousands of square kilometers; so the resulting climate projections from GCMs cannot be directly used as input for models at the resolution of interest to hydrologists (Epstein and Ramírez, 1994; Morrison et al., 2002). Consequently, various downscaling techniques that include stochastic, statistical, or dynamic downscaling (Fowler et al., 2007; Maurer et al., 2009; Wang et al., 2011) have been developed to derive higher resolution climate data from the coarser resolution climate projections. Dynamic downscaling refers to the use of regional climate models (RCMs) (Fowler et al., 2007; Mehrotra and Sharma, 2010). Catchment scale hydrological climate change impact studies have used dynamically downscaled output (e.g. Fowler and Kilsby, 2007; Wood et al., 2004), simple statistical approaches such as multiple regression relationships (e.g. Jasper et al., 2004; Wilby et al., 2000), and stochastic weather generator (e.g. Evans and Schreider, 2002).

Potential impacts of future climate change on hydrology have been assessed through the application of hydrological models driven by the downscaled GCM derived future climates (Campbell et al., 2011; Forbes et al., 2011; Kienzle et al., 2012; Loukas et al., 2002; Toth et al., 2006). A detailed, physically based model could be an effective tool; however, applying a detailed model may require large numbers of input forcing which are seldom available, especially in mountain region studies. So, the selection of the model may depend on the availability of data for the study region.

The purpose of this study is to evaluate the effects of potential future climate and forest changes on the high water yielding headwaters of Alberta's eastern slopes, focusing on southern portions that supply the overwhelming majority of useable surface water for communities. These Mountain regions are more susceptible to future temperature change as a large proportion of the precipitation falling in these regions is





HESSD
10, 8503–8536, 2013

snow which will partly change to rain in a warming climate thereby affecting the timing and magnitude of streamflow (Forbes et al., 2011; Kienzle et al., 2012). In this study we include high mountains and examine the possible compounding impacts of forest change.

## 2 Study watershed and data

The Crowsnest Creek watershed (Fig. 1), centred at 49.64° N, 114.55° W, is an important watershed in Southern Alberta, Canada. It feeds the Oldman River which is closed to the issuing of new water extraction licenses due to a growing imbalance between demand and supply (Emelko et al., 2011). This watershed has a drainage area of 384 $km^2$ with the elevation ranging from 1236 to 2732 m. The watershed is broadly characteristic of Rocky Mountain front-range physiographic settings. Vegetation in the watershed is characterized by Lodgepole pine (Pinus contorta Dougl. ex Loud. Var. latifolia Engelm.) dominated forest at lower elevations, subalpine forest at mid elevations dominated by Engelmann spruce (Picea engelmannii Parry ex Englem.) and subalpine fir (Abies lasiocarpa [Hook.] Nutt.) with alpine ecozones at higher elevations characterized by alpine meadow vegetation and bare rock extending above tree line (Silins et al., 2009).

The majority of the total annual precipitation (50 to 70 %) in these catchments falls as snow from October to April. Streamflows in the study area are characteristic of very high water yielding Rocky Mountain streams. Spring snowmelt generally produces the highest continuous streamflows. Rain-on-snow or mid-winter melt events are a common occurrence, producing some of the larger flows, with mean daily discharge in excess of 30 mm $day^{-1}$. The late summer and over winter period are generally near 0.5–2 mm $day^{-1}$ (Silins et al., 2009). Hydrology of all these catchments are snowmelt dominated and peak flows are driven by spring snowmelt or rain on spring snowmelt.

Climate has been monitored continuously by seven climate stations within this watershed by Environment Canada (http://climate.weatheroffice.gc.ca/climateData/canada_





HESSD
10, 8503–8536, 2013

Impacts of climate and forest changes on streamflow

V. Mahat and A. Anderson

e.html). However, a long record of climate data (i.e. about 32 yr, from 1965 to 1997) is available only at the Coleman climate station which lies at the approximate centre of the watershed (Fig. 1). We use climate data recorded at this station to drive the daily climatological condition across the entire watershed, herein called the Coleman climate station. Streamflow data used in this study are the data recorded at the gauging station on the Crowsnet River at Frank (Hydat Station: 05AA008), located close to the city of Blairmore, AB. This station is well suited for the analysis as long-term records of streamflow data, which are necessary for calibrating and validating the model that simulates the effect of climate change on streamflow, are available at this station.

## 3 Methodology

The study methodology to assess the climate change impacts on streamflow involves three steps:

1. develop estimates of future monthly climate means (precipitation, maximum temperature $T_{max}$, and minimum temperature, $T_{min}$) in relation to observed (reference) climates at the Coleman climate station;

2. disaggregate (temporal downscale) monthly climate means into daily realizations for use with the hydrological model; and

3. hydrological model calibration, application and parameter uncertainty.

### 3.1 Estimates of future monthly climate means

Projected monthly climate means used in this study are GCM outputs that are downscaled to 1 × 1 km grids using the climateWNA model (Wang et al., 2006, 2011). ClimateWNA uses a combination of bilinear interpolation and elevation adjustment to downscale the climate data. GCM used in this study is the Canadian Climate Centre's Modeling and analysis (CCCma) third generation coupled global climate model





HESSD
10, 8503–8536, 2013

(CGCM3) (http://www.ec.gc.ca/ccmac-cccma/default.asp?lang=En&n=4A642EDE-1). ClimateWNA downscaled 1x1 km grids from within the study watershed boundary are averaged to estimate the watershed averaged monthly climate means for reference and future periods, and changes in monthly climate means, (i.e. change in mean monthly daily maximum temperature, $\Delta T_{\max}$, change in mean monthly daily minimum temperature, $\Delta T_{\min}$ and change in monthly precipitation, $\Delta P$) are calculated as

$$\Delta T_{\max} = \left(T^{F}_{\max} + \varepsilon\right) - \left(T^{R}_{\max} + \varepsilon\right) \tag{1}$$

$$\Delta T_{\min} = \left(T^{F}_{\min} + \varepsilon\right) - \left(T^{R}_{\min} + \varepsilon\right) \tag{2}$$

$$\Delta P = \frac{\varepsilon P^{F}}{\varepsilon P^{R}} \tag{3}$$

where, $T^{R}_{\max}$, $T^{R}_{\min}$ and $P^{R}$ are watershed averaged mean monthly daily maximum temperature, mean monthly daily minimum temperature and monthly precipitation, respectively for the reference period, and $T^{F}_{\max}$, $T^{F}_{\min}$ and $P^{F}$ are watershed averaged mean monthly daily maximum temperature, mean monthly daily minimum temperature and monthly precipitation, respectively for the future period. $\varepsilon$ is the bias.

The reference period used in this study is between 1965 and 1997, chosen because of the observed daily climates available for the hydrological model calibration and validation during this period. Future periods selected are anomalies for 30 yr normal periods 2011–2040 (2020s), 2041–2070 (2050s), and 2071–2100 (2080s). Three emission scenarios (A1B, A2, and B1) that were developed utilizing the intergovernmental Panel on Climate Change (IPCC) Fourth Assessment Report, AR4 are used. The A1B scenario describes “a future world of very rapid economic growth, global population that peaks in mid-century and declines thereafter, and rapid introduction of new and more efficient technologies”. The A2 scenario describes “economic development is primarily regionally oriented and per capita economic growth and technological change are more fragmented and slower compared to A1B and B1 scenarios”; and the B1 scenario describes “a convergent world with the same global population that peaks in mid-century and declines thereafter, as in the A1 storyline, but with rapid changes in economic structures toward a service and information economy, with reductions in material intensity, and the introduction of clean and resource-efficient technologies" (IPCC, 2007).

We assume the relative changes in monthly climate means at the Coleman climate station is equivalent to the changes in watershed averaged monthly climate means, $\Delta T_{max}$, $\Delta T_{min}$ and $\Delta P$ that are obtained from Eqs. (1)–(3). Daily observed climate at Coleman is aggregated to a monthly scale and perturbed with these $\Delta T_{max}$, $\Delta T_{min}$ and $\Delta P$ to give future monthly climate means at the Coleman climate station.

### 3.2 Disaggregation

A weather generator can be used to disaggregate monthly climate means into daily realizations for use with a hydrological model (Richardson and Wright, 1984). Weather generators are stochastic numeric models that simulate daily weather data at a single site using the separate statistical properties for each month's observed daily weather data for the given site (Racsko et al., 1991; Richardson et al., 1998; Semenov and Brooks, 1999). There are two types of daily weather generators used to determine wet or dry days and precipitation amount. Wet days are days with precipitation larger than zero. The first type, the Markov chain approach, uses a two state first order Markov chain to generate wet or dry days using a random process conditional upon the state of the previous day (Hughes et al., 1999). If a day is determined as wet, then the precipitation amount is computed using two-parameter gamma distribution. The second type, spell-length approach, generates wet or dry series. The length of each series is chosen randomly from the wet and dry semi-empirical distribution for the month in which the series starts (Racsko et al., 1991; Wilks, 2012). The wet day precipitation value is generated using a semi-empirical precipitation distribution independent of the length of the wet series or the amount of precipitation on previous days (Semenov and Brooks, 1999).

We use the Long Ashton Research Station Weather Generator (LARS-WG) that uses a more flexible semi-empirical approach compared to the Markov chain approach





HESSD
10, 8503–8536, 2013

which uses a simple standard distribution to generate a series of wet and dry days. In LARS-WG, daily $T_{max}$ and $T_{min}$ are modeled separately as stochastic processes with daily means and standard deviation conditioned on the wet or dry status of the day (Semenov and Brooks, 1999). The seasonal cycles of means and standard deviations are modeled by finite Fourier series of order 3 which is constructed using observed mean values, sine and cosine curve and phase angle for each month. LARS-WG also uses autocorrelation values for $T_{min}$ and $T_{max}$ derived from observed weather data to model the temperature. LARS-WG is available to the broader climate change impact study community via the Environment Canada web site (http://www.cccsn.ec.gc.ca/index.php?page=lars-wg).

Monthly statistical parameters of climates observed at the Coleman climate station are extracted using LARS-WG, and a new set of daily climates for the reference period 1965–1997 are generated. These generated climates are compared with the observed climates at the Coleman climate station to evaluate the performance of LARS-WG. Once reference climates are generated and validated, nine sets (for three different scenarios: A1B, A2 and B1, and for three different time periods: 2020s, 2050s and 2080s) of future periods daily climates are generated disaggregating the future monthly climate means estimated for Coleman station. Although observed daily climates are available for the reference period, we use stochastically generated climates to provide input to the hydrological model to simulate the reference period streamflow. This makes the reference and future period streamflows comparable because they are generated with the same methods, but reflect the statistical properties of the climate periods.

## 3.3 Hydrological model calibration, application and parameters uncertainty

### 3.3.1 HBV-EC

A common conceptual hydrological model, HBV-EC is used to study the hydrological impacts of climate change. HBV-EC is a version of the conceptual HBV model (Bergstrom and Forsman, 1973; Lindström et al., 1997) that simulates daily/hourly discharge using daily/hourly precipitation and temperature and monthly estimates of evapotranspiration as input. The model is based on the concept of grouped response units (GRUs) that groups together DEM/GIS grid cells having similar elevation, aspect, slope and land cover. HBV-EC uses elevation bands subdivided into different land types (open, forest, glacier and water), slopes and aspects. Lateral climate gradients in HBV-EC are represented by subdividing the basin into different climate zones; each of which is associated with a climate station and a unique set of parameters (Jost et al., 2012). The model consists of three main modules: (1) a snow module that simulates snow accumulation and melt using a degree-day approach; (2) a soil module that simulates groundwater recharge and actual evaporation as functions of soil moisture; and (3) a runoff transfer module that consists of one upper nonlinear reservoir representing fast responses and one lower linear reservoir representing slow responses to delay the runoff in time. Detailed descriptions of HBV-EC are given by Hamilton et al. (2000). HBV-EC is an open source, available at the modeling framework 'Green Kenue' (http://www.nrc-cnrc.gc.ca/eng/solutions/advisory/green_kenue/downloadgreenkenue.html) developed by the National Research Council Canada in collaboration with Environment Canada.

### 3.3.2 Hydrological model calibration

The HBV-EC model is driven by the thirty two years (1965–1997) of climate data recorded at the Coleman climate station to simulate the streamflow which is compared with observed flow at Frank. The watershed is divided into five different elevation zones which are further divided into different land use types, slope and aspects. Temperature and precipitation lapse rates within the watershed are calculated using the climateWNA generated monthly climate data. The model was calibrated using the optimization algorithm Genoud (written in the rgenoud R application; Mebane and Sekhon, 2011) that combines evolutionary algorithm methods with steepest gradient descent algorithm (Jost et al., 2012) to maximize the Nash-Sutcliffe efficiency (NSE) (Nash and Sutcliffe, 1970) of the streamflow.





HESSD
10, 8503–8536, 2013



V. Mahat and A. Anderson

### 3.3.3 Application

The calibrated model is then driven by the LARS-WG generated daily climates to simulate the streamflows for reference and future periods. Reference period model simulated streamflow is compared with observed flow to determine how well the LARS-WG generated climate can represent the properties of the observed streamflow. Simulated streamflows for the reference and future periods are compared to assess the climate change impacts.

### 3.3.4 Parameter uncertainty

In HBV-EC model parameters can be interdependent, and different parameter sets can produce good results (high NSE) for one period but not for another (Beven, 2000; Seibert et al., 2010; Steele-Dunne et al., 2008). To address this problem of parameter uncertainty, a Monte Carlo technique was employed and 100 most efficient model parameter sets that result in NSE values higher than those obtained from the Genoud, minus a threshold, are selected. These 100 parameter sets are used with HBV-EC to provide a range of model results to help understand the model sensitivity to the parameter uncertainties.

### 3.3.5 Forest change

A change detection modeling technique suggested by Seibert and McDonnel (2010) and Seibert et al. (2010) is used to assess the impacts of forest change on the streamflow. Seibert et al. (2010) used a similar hydrological model to quantify the impacts on streamflow after forest removal from a watershed due to wildfire. We remove forest from the watershed and run HBV-EC for reference and future periods to understand how removal of forest in reference and future periods would impact the streamflow.

## 4 Results

### 4.1 Estimates of future monthly climate means

Relative changes in watershed averaged monthly climate means observed in GCM outputs for nine different future scenarios are in Table 1. GCM projections showed an increase in precipitation during winter (December, January and February) and a decrease in precipitation during summer (June, July and August) in our watershed. Projections for spring (March, April and May) and fall (September, October and November) were mixed. There was a consistent increase in mean temperature for all seasons of the year (Table 1).

Future monthly climate means (precipitation, $T_{max}$ and $T_{min}$) at the Coleman climate station for the nine scenarios, along with the reference period observed climate aggregated to monthly scale, are presented in Fig. 2. Disaggregation of these provides climate inputs to the hydrological model to simulate reference and future periods streamflows. Figure 2 shows higher precipitation during winter and lower precipitation during summer for future periods in comparison to the reference period. However, the increase or decrease in future periods precipitation compared to reference period was less than 10 % for any seasons. $T_{max}$ and $T_{min}$ for future periods are higher for all seasons.

### 4.2 Disaggregation

LARS-WG model performance was evaluated by comparing the observed and LARS-WG generated means and variances for monthly precipitation by using $t$ and $f$ test, respectively and means of daily $T_{max}$ and $T_{min}$ by using the $t$ test (Table 2). LARS-WG reproduced 100 % (for all twelve months) monthly means for precipitation giving $p$ values higher than 0.05 suggesting that there is not a significant difference in means at the 95 % confidence level as shown in Table 2. However, only 75 % of monthly variances for precipitation were reproduced by the model (4 out of 12 $p$ values for the $f$ test are less than 0.05). LARS-WG produced mixed results for $T_{min}$ and $T_{max}$. The $t$ tests for the





HESSD
10, 8503–8536, 2013

$T_{min}$ were significant for 4 months out of 12 (4 out of 12 $p$ values for the $t$ test are less than 0.05) and the $t$ tests for the $T_{max}$ were significant for 2 months out of 12 months (2 out of 12 $p$ values for the $t$ test are less than 0.05). Comparison of LARS-WG simulated mean monthly precipitation and monthly mean values of daily $T_{max}$ and $T_{min}$ with observed climates are presented in Fig. 3.

### 4.3 HBV-EC calibration

Figure 4 compares the observed daily streamflow at the watershed outlet, Crowsnest at Frank, with HBV-EC simulated values for the calibration period 1965–1997. Both high and low flows were simulated reasonably well, except few larger peaks that were underestimated by the model (Fig. 4). NSE of 0.82 was obtained during this calibration period. Differences in mean monthly streamflow between the observed and simulated values range from −15 to 50 %. The largest difference observed was during the month of February. Though the difference was large in percentage, in terms of magnitude the difference was very small, about 5 mm. A maximum of 12 mm difference was observed in the month of June. Differences between the observed and simulated annual flows range from −25 to 40 %. The largest differences (> |15 %|) observed were during the years 1968, 1969, 1973, 1974,1988, 1991 and 1994. In other years the differences were less than 15 %. While there were discrepancies in the simulated versus observed mean monthly and annual flows, the negative and positive errors offset each other giving only 6 % (about 25 mm) difference in mean annual flow between the observed and simulated values.

### 4.4 HBV-EC application

Figure 5 compares the model simulated streamflow (daily, monthly and annual) with the observed streamflow values at the study watershed outlet, Crowsnest at Frank. Input to the HBV-EC in this case is LARS-WG generated daily realizations. Daily, monthly and annual comparisons (Fig. 5) show that the simulated streamflow are realistic and





HESSD
10, 8503–8536, 2013



V. Mahat and A. Anderson

close to the observed values as in Fig. 4. However, the NSE was not that great. This is somewhat expected given that the generated weather data captures the stats but not the actual amounts.

Figure 6 compares the HBV-EC simulated streamflows at the watershed outlet, Crowsnest at Frank, for the reference period and nine future periods. Mean monthly hydrographs of all future simulations (Fig. 6) showed an early initiation of peaks resulting in the seasonal shift, a shift toward higher spring (March, April) flows and a corresponding decrease in summer (June and July) flows associated with the shift in the spring flows compared to the reference period hydrographs. Future simulations also showed an increase in the winter low flows. Winter low flows increased up to 200 % (9.3 mm) in February while summer high flows decreased up to 63 % (31.2 mm) in June in the A2 scenario in the 2080s time period. Fall (September, October and November) flows were affected less and remained almost the same for all future periods. Despite the variations in the mean monthly flows, mean annual flows for the reference and future periods were quite similar (Fig. 6). Maximum increase in mean annual flow was projected to be approximately 9 % in the 2080s for the A2 scenario while the maximum decrease was projected to be approximately 6 % in the 2050s for the A1B scenario.

The reference and future periods mean monthly snow water equivalent (SWE) and mean monthly evapotranspiration for the study watershed are presented in Fig. 7. SWE values decreased in all future simulations. Evapotranspiration increased in spring and decreased in summer. Despite an increase in temperature throughout the year, a decrease in evapotranspiration during the summer indicates a water deficit during the summer.

### 4.5 Parameter uncertainty

Relative changes in mean monthly streamflows in different future periods compared to the reference period were calculated from the HBV-EC ensemble simulations (Fig. 8). Ensemble spread was found to be higher in spring and summer than in winter and fall in all future scenarios indicating higher parameter uncertainty impacts on spring and





HESSD
10, 8503–8536, 2013

summer flows than on winter and fall flow. Single simulation showed maximum of about 31.2 mm of streamflow reduction during summer while the ensemble showed up to an 80 mm reduction in streamflow in summer. The ensemble mean showed approximately a 46 mm reduction in summer flow which is about 1.5 times higher than what the single simulation predicted.

### 4.6 Forest change

Ensemble streamflows were generated using the best 100 parameter sets to assess the forest change impacts to the streamflow in the reference and future periods. Forest change impact assessed for the future period is the combined forest and the climate change impacts. The worst case climate condition: 2080s with A2 climate scenario, was combined with forest change scenario to represent the possible worst case future scenario. Figure 9a–c show relative changes in mean monthly streamflow (ensemble and mean) due to forest removal (Fig. 9a), due to climate change (Fig. 9b), and due to combined forest removal and climate change (Fig. 9c). Mean values of these ensembles are also compared in Fig. 9d. The removal of forest from the watershed increased the streamflow in early spring, late summer and early fall, and reduced the streamflow in late spring and early summer. The mean ensemble (Fig. 9d) shows a higher increase in winter flow due to the combined forest removal and climate change impact compared to an individual impact produced by forest removal or climate change. However, the combined impact on the summer flow was less compared to the climate only change impact, suggesting that the forest had a role in the summer evapotranspiration and streamflow.

## 5 Discussion

This study uses GCM outputs downscaled using the ClimateWNA model with two other models: LARS-WG and HBV-EC to assess the impacts of climate and forest changes





HESSD
10, 8503–8536, 2013



V. Mahat and A. Anderson

on streamflow. These types of studies inherently have large sources of uncertainty in predictions and are used to inform trends rather provide predictive results. Inclusion of uncertainty estimates in GCM simulations, ClimateWNA downscaling or and LARS- WG disaggregation may provide the robust assessment of the impacts of climate change on water resource systems. However, analyses of uncertainty in the climate simulations and downscaling are beyond the scope of this study. Uncertainty in the LARS-WG disaggregation and hydrological modeling are analyzed and partly taken into account.

LARS-WG reproduced monthly means and variances for the precipitation very well; however it demonstrated a relatively poor performance especially in reproducing the monthly variances of $T_{max}$ and $T_{min}$. Results were mixed in reproducing means of $T_{max}$ and $T_{min}$. The possible source of error could be the use of many pre-set values in the model. While estimating an average daily standard deviation for $T_{max}$ and $T_{min}$, LARS-WG normalises the temperature residuals using constant auto-correlations and cross-correlations between the temperature residuals through the year. Those constant values are site specific and might be different for our climate. Semenov and Brooks (1999) recommend site specific testing and validation of the model before the generated data are used in a sensitive application, where more accuracy is required for each variable, for example, in a study of an extreme weather event. For this study LARS-WG can be implemented without any changes in the model. Although the model did not reproduce the variances very well, it reproduced the average behaviour of observed data and so the performance for mean precipitation and temperature was good.

The hydrological model used in this study is a conceptual model and does not represent many physical processes. However, the choice was governed by the availability of data. Observed climate and other data available for model input and verification were limited. Although there are some climate stations at higher elevations, their records were short and seasonal. More detailed models may represent the physical processes thoroughly, but use of these models under such conditions may cause problems of over-parameterization, parameter estimation and validation limitations.





HESSD
10, 8503–8536, 2013

HBV-EC reasonably captured the reference period daily streamflow with NSE 0.82 as well as monthly and annual flow very well. Streamflow simulated using LARS-WG generated climates also matched the daily, monthly and annual observed streamflow reasonably, though the NSE value was low and model error was large. However, the error that LARS-WG produced is inherent and would be consistent in both reference and future period simulations and would not affect much in the evaluation of climate and forest change impacts.

The hydrological model in this study was calibrated against the streamflow measurements only. It would have been better if we were able to calibrate the model against other measurements, i.e. SWE, soil moisture content or evapotranspiration before the model was used to simulate future streamflows but the limited data did not afford the luxury to validate the model against other measurements.

Comparison of HBV-EC simulated flows for the reference and future periods in climate change studies suggest an amplification of the seasonal cycle with increased winter precipitation leading to a rise in winter (DJF) stream flow. Increase in streamflow during the winter could have been caused by the partial replacement of snowfall by rainfall due to the increase in temperature during the season when potential evapotranspiration rates are low (Forbes et al., 2011). The combination of increased temperature and decreased precipitation resulted in reduction in May and summer (JJA) streamflow. Previous climate change studies carried out in similar regions in Canada (e.g. Dibike and Coulibaly, 2005; Forbes et al., 2011; Kienzle et al., 2012) have also found increased streamflows in winter and spring, and decreased streamflows in summer. We found that these changes (increased or decreased streamflow) were relatively higher for the A2 climate scenario, which is reflective of the largest changes to climate when compared to the other two scenarios.

The model parameter uncertainty analysis showed that streamflow predictions vary considerably. The higher spread observed in ensemble simulations in summer indicates a higher risk of lower summer flows than was predicted by the single simulation. Combined climate and forest change impacts compounded the effect of increasing





HESSD
10, 8503–8536, 2013



V. Mahat and A. Anderson

Title Page
Abstract | Introduction
Conclusions | References
Tables | Figures
◂◂ | ▸▸
◂ | ▸
Back | Close
Full Screen / Esc
Printer-friendly Version
Interactive Discussion

winter flow; however, it did not reduce the summer flow very much. The higher winter or early spring flow in both reference and future periods observed after removal of forest may be caused by the quicker snowmelt when forest was removed. Usually the removal of forest results in increased summer flow due to less evapotranspiration during the summer or fall. In our case the model does not distinguish the difference in evapotranspiration based on the presence or absence of the forest, thus the less reduction in the simulation of summer flow when forest was removed is possibly due to the higher soil moisture recharge during the winter that resulted in higher soil moisture release during the summer.

## 6 Conclusions

A watershed in the eastern slopes of the Southern Alberta Rocky Mountains was modeled to investigate the potential impacts of climate and forest changes on its hydrology using a simple conceptual hydrological model, HBV-EC. Monthly climate data downscaled to 1 × 1 km grids are disaggregated to daily realizations using a stochastic weather generator, LARS-WG. These realizations provided the inputs to the HBV-EC to simulate reference and future scenarios streamflows that are compared to assess the climate and forest change impacts. Climate change impacts are mainly observed in the seasonality of streamflow: higher winter flows and lower summer flows. These are mainly caused by the increase in temperature as there was not much difference in precipitation between reference and future periods. Summer flows were found to be more vulnerable and the consequences are less availability of summer water in the river which is already stressed due to higher demand than supply. The use of an ensemble of parameter sets in this study allowed us to examine the impact of parameter uncertainty in the streamflow simulations. However, uncertainties exist in model simulations of many hydrologic components (i.e. soil moisture, base flow, snow accumulation and ablation, evapotranspiration etc.) that are not validated in this study. Poor





HESSD
10, 8503–8536, 2013



V. Mahat and A. Anderson

representations of these may largely affect the model results in the simulations of future streamflows for climate change studies.

*Acknowledgements.* This research was supported by Alberta Innovates – Bio Solutions. We are especially grateful to Mike Wagner, Chris Williams and Amanda Martens for technical assistance.

## References

Arnell, N. W.: Climate change and global water resources, Global Environ. Change, 9, S31–S49, doi:10.1016/S0959-3780(99)00017-5, 1999.

Barnett, T. P., Adam, J. C., and Lettenmaier, D. P.: Potential impacts of a warming climate on water availability in snow-dominated regions, Nature, 438, 303–309, 2005.

Barnett, T. P., Pierce, D. W., Hidalgo, H. G., Bonfils, C., Santer, B. D., Das, T., Bala, G., Wood, A. W., Nozawa, T., Mirin, A. A., Cayan, D. R., and Dettinger, M. D.: Human-induced changes in the hydrology of the Western United States, Science, 319, 1080–1083, doi:10.1126/science.1152538, 2008.

Bergstrom, S. and Forsman, A.: Development of a conceptual deterministic rainfall-runoff model, Nord. Hydrol., 4, 147–170, 1973.

Beven, K. J.: Rainfall Runoff Modelling: The Primer, John Wiley, Chichester, 2000.

Bladon, K. D., Silins, U., Wagner, M. J., Stone, M., Emelko, M. B., Mendoza, C. A., Devito, K., and Boon, S.: Wildfire and salvage logging impacts on nitrogen export from headwater streams in southern Alberta's Rocky Mountains, Can. J. Forest. Res., 38, 2359–2371, 2008.

Campbell, J. L., Driscoll, C. T., Pourmokhtarian, A., and Hayhoe, K.: Streamflow responses to past and projected future changes in climate at the Hubbard Brook Experimental Forest, New Hampshire, United States, Water Resour. Res., 47, W02514, doi:10.1029/2010wr009438, 2011.

Dibike, Y. B. and Coulibaly, P.: Hydrologic impact of climate change in the Saguenay watershed: comparison of downscaling methods and hydrologic models, J. Hydrol., 307, 145–163, doi:10.1016/j.jhydrol.2004.10.012, 2005.

Emelko, M. B., Silins, U., Bladon, K. D., and Stone, M.: Implications of land disturbance on drinking water treatability in a changing climate: Demonstrating the need for "source water supply





HESSD
10, 8503–8536, 2013

and protection" strategies, Water Res., 45, 461–472, doi:10.1016/j.watres.2010.08.051, 2011.
Epstein, D. and Ramírez, J.: Spatial disaggregation for studies of climatic hydrologic sensitivity, J. Hydraul. Eng.-ASCE, 120, 1449–1467, doi:10.1061/(ASCE)0733-9429(1994)120:12(1449), 1994.
Evans, J. and Schreider, S.: Hydrological impacts of climate change on inflows to Perth, Australia, Climatic Change, 55, 361–393, doi:10.1023/a:1020588416541, 2002.
Forbes, K., Kienzle, S., Coburn, C., Byrne, J., and Rasmussen, J.: Simulating the hydrological response to predicted climate change on a watershed in southern Alberta, Canada, Climatic Change, 105, 555–576, doi:10.1007/s10584-010-9890-x, 2011.
Fowler, H. J. and Kilsby, C. G.: Using regional climate model data to simulate historical and future river flows in northwest England, Climatic Change, 80, 337–367, doi:10.1007/s10584-006-9117-3, 2007.
Fowler, H. J., Blenkinsop, S., and Tebaldi, C.: Linking climate change modelling to impacts studies: recent advances in downscaling techniques for hydrological modelling, Int. J. Climatol., 27, 1547–1578, doi:10.1002/joc.1556, 2007.
Hamilton, A. S., Hutchinson, D. G., and Moore, R. D.: Estimating winter streamflow using conceptual streamflow model, J. Cold Reg. Eng., 14, 158–175, 2000.
Hamlet, A. F. and Lettenmaier, D. P.: Effects of climate change on hydrololgy and water resources in the Columbia River Basin, J. Am. Water Ressour. Assoc., 35, 1597–1623, doi:10.1111/j.1752-1688.1999.tb04240.x, 1999.
Hidalgo, H. G., Das, T., Dettinger, M. D., Cayan, D. R., Pierce, D. W., Barnett, T. P., Bala, G., Mirin, A., Wood, A. W., Bonfils, C., Santer, B. D., and Nozawa, T.: Detection and attribution of streamflow timing changes to climate change in the Western United States, J. Climate, 22, 3838–3855, doi:10.1175/2009jcli2470.1, 2009.
Hughes, J. P., Guttorp, P., and Charles, S. P.: A non-homogeneous hidden Markov model for precipitation occurrence, J. R. Stat. Soc., 48, 15–30, doi:10.1111/1467-9876.00136, 1999.
IPCC: Contribution of Working Groups I, II and III to the Fourth Assessment Report of the Intergovernmental Panel on Climate Change, edited by: Core Writing Team: Pachauri, R. K. and Reisinger, A., IPCC, Geneva, Switzerland, 104 pp., 2007.
Jasper, K., Calanca, P., Gyalistras, D., and Fuhrer, J.: Differential impacts of climate change on the hydrology of two alpine river basins, Clim. Res., 26, 113–129, doi:10.3354/cr026113, 2004.

Jha, M., Pan, Z., Takle, E. S., and Gu, R.:, Impacts of climate change on streamflow in the Upper Mississippi River Basin: A regional climate model perspective, J. Geophys. Res., 109, D09105, doi:10.1029/2003jd003686, 2004.
Jost, G., Moore, R. D., Menounos, B., and Wheate, R.: Quantifying the contribution of glacier runoff to streamflow in the upper Columbia River Basin, Canada, Hydrol. Earth Syst. Sci., 16, 849–860, doi:10.5194/hess-16-849-2012, 2012.
Kienzle, S. W., Nemeth, M. W., Byrne, J. M., and MacDonald, R. J.: Simulating the hydrological impacts of climate change in the upper North Saskatchewan River basin, Alberta, Canada, J. Hydrol., 412–413, 76–89, doi:10.1016/j.jhydrol.2011.01.058, 2012.
Lindström, G., Johansson, B., Persson, M., Gardelin, M., and Bergström, S.:, Development and test of the distributed HBV-96 hydrological model, J. Hydrol., 201, 272–288, doi:10.1016/S0022-1694(97)00041-3, 1997.
Loukas, A., Vasiliades, L., and Dalezios, N. R.: Potential climate change impacts on flood producing mechanisms in southern British Columbia, Canada using the CGCMA1 simulation results, J. Hydrol., 259, 163–188, doi:10.1016/S0022-1694(01)00580-7, 2002.
Maurer, E. P., Adam, J. C., and Wood, A. W.: Climate model based consensus on the hydrologic impacts of climate change to the Rio Lempa basin of Central America, Hydrol. Earth Syst. Sci., 13, 183–194, doi:10.5194/hess-13-183-2009, 2009.
Mebane, W. R. and Sekhon, J. S.: Genetic optimization using derivatives: The rgenoud package for R, J. Stat. Softw., 42, 1–26, 2011.
Mehrotra, R. and Sharma, A.: Development and application of a multisite rainfall stochastic downscaling framework for climate change impact assessment, Water Resour. Res., 46, W07526, doi:10.1029/2009wr008423, 2010.
Morrison, J., Quick, M. C., and Foreman, M. G. G.: Climate change in the Fraser River watershed: flow and temperature projections, J. Hydrol., 263, 230–244, doi:10.1016/S0022-1694(02)00065-3, 2002.
Mote, P. W.: Trends in snow water equivalent in the Pacific Northwest and their climatic causes, Geophys. Res. Lett., 30, 1601, doi:10.1029/2003gl017258, 2003.
Nash, J. E.,and Sutcliffe, J. V.: River flow forecasting through conceptual models, part 1, A discussion of principles, J. Hydrol., 10, 282–290, 1970.
Pierce, D. W., Barnett, T. P., Hidalgo, H. G., Das, T., Bonfils, C., Santer, B. D., Bala, G., Dettinger, M. D., Cayan, D. R., Mirin, A., Wood, A. W., and Nozawa, T.: Attribution of declining Western





HESSD
10, 8503–8536, 2013

U.S. snowpack to human effects, J. Climate, 21, 6425–6444, doi:10.1175/2008jcli2405.1, 2008.
Racsko, P., Szeidl, L., and Semenov, M.: A serial approach to local stochastic weather models, Ecol. Model., 57, 27=-41, doi:10.1016/0304-3800(91)90053-4, 1991.
Richardson, C. W. and Wright, D. A.: WGEN: A model for generating daily weather variables, US Dept. of Agriculture, ARS-8, USDA, Washington, D.C., 1984.
Richardson, C. W., Barrow, E. M., and Semenov, M. A.: Comparison of the WGEN and LARS-WG stochastic weather generators in diverse climates, Clim. Res., 10, 95–107, 1998.
Seibert, J. and McDonnell, J. J.: Land-cover impacts on streamflow: a change-detection modelling approach that incorporates parameter uncertainty, Hydrolog. Sci. J., 55, 316–332, doi:10.1080/02626661003683264, 2010.
Seibert, J., McDonnell, J. J., and Woodsmith, R. D.: Effects of wildfire on catchment runoff response: a modelling approach to detect changes in snow-dominated forested catchments, Hydrol. Res., 41, 378–390, doi:10.2166/nh.2010.036, 2010.
Semenov, M. A. and Brooks, R. J.: Spatial interpolation of the LARS-WG stochastic weather generator in Great Britain, Clim. Res., 11, 137–148, 1999.
Silins, U., Stone, M., Emelko, M. B., and Bladon, K. D.: Sediment production following severe wildfire and post-fire salvage logging in the Rocky Mountain headwaters of the Oldman River Basin, Alberta, Catena, 79, 189–197, doi:10.1016/j.catena.2009.04.001, 2009.
Stahl, K., Moore, R. D., Shea, J. M., Hutchinson, D., and Cannon, A. J.: Coupled modelling of glacier and streamflow response to future climate scenarios, Water Resour. Res., 44, W02422, doi:10.1029/2007wr005956, 2008.
Steele-Dunne, S., Lynch, P., McGrath, R., Semmler, T., Wang, S., Hanafin, J., and Nolan, P.: The impacts of climate change on hydrology in Ireland, J. Hydrol., 356, 28–45, doi:10.1016/j.jhydrol.2008.03.025, 2008.
Stone, M. C., Hotchkiss, R. H., Hubbard, C. M., Fontaine, T. A., Mearns, L. O., and Arnold, J. G.: Impacts of climate change on Missouri River Basin water yield, J. Am. Water Resour. Assoc., 37, 1119–1129, doi:10.1111/j.1752-1688.2001.tb03626.x, 2001.
Toth, B., Pietroniro, A., Conly, F. M., and Kouwen, N.: Modelling climate change impacts in the Peace and Athabasca catchment and delta: I – hydrological model application, Hydrol. Process., 20, 4197–4214, doi:10.1002/hyp.6426, 2006.





HESSD
10, 8503–8536, 2013

Impacts of climate and forest changes on streamflow

V. Mahat and A. Anderson

Wang, T., Hamann, A., Spittlehouse, D. L., and Aitken, S. N.: Development of scale-free climate data for western Canada for use in resource management, Int. J. Climatol., 26, 383–397, 2006.

Wang, T., Hamann, A., Spittlehouse, D. L., and Murdock, T. Q.: ClimateWNA – high-resolution spatial climate data for Western North America, J. Appl. Meteorol. Clim., 51, 16–29, doi:10.1175/JAMC-D-11-043.1, 2011.

Wilby, R. L., Hay, L. E., Gutowski, W. J., Arritt, R. W., Takle, E. S., Pan, Z., Leavesley, G. H., and Clark, M. P.: Hydrological responses to dynamically and statistically downscaled climate model output, Geophys. Res. Lett., 27, 1199–1202, doi:10.1029/1999gl006078, 2000.

Wilks, D. S.: Stochastic weather generators for climate-change downscaling, part II: multivariable and spatially coherent multisite downscaling, WIREs Clim. Chang., 3, 267–278, doi:10.1002/wcc.167, 2012.

Wood, A. W., Leung, L. R., Sridhar, V., and Lettenmaier, D. P.: Hydrologic implications of dynamical and statistical approaches to downscaling climate model outputs, Climatic Change, 62, 189–216, doi:10.1023/B:CLIM.0000013685.99609.9e, 2004.

Zheng, H., Zhang, L., Zhu, R., Liu, C., Sato, Y., and Fukushima, Y.: Responses of streamflow to climate and land surface change in the headwaters of the Yellow River Basin, Water Resour. Res., 45, W00A19, doi:10.1029/2007wr006665, 2009.





HESSD

10, 8503–8536, 2013



V. Mahat and A. Anderson

Title Page
Abstract | Introduction
Conclusions | References
Tables | Figures
◀| |▶
◀ ▶
Back | Close
Full Screen / Esc
Printer-friendly Version
Interactive Discussion

**Table 1.** Relative changes in watershed averaged mean monthly GCM projections of precipitation and air temperature for A1B, A2 and B1 scenario for 2020s, 2050s, and 2080s time periods.

| Time period | Scenario | Jan | Feb | Mar | Apr | May | Jun | Jul | Aug | Sep | Oct | Nov | Dec | Annual | Annual mean |
|---|---|---|---|---|---|---|---|---|---|---|---|---|---|---|---|
| Percentage change in mean monthly precipitation, $\Delta P$ | | | | | | | | | | | | | | | |
| 2011–2040 (“2020s”) | A1B | 2.6 | 4.1 | −4.3 | 3.9 | −7.3 | −5.0 | −2.4 | −2.8 | 3.2 | −2.7 | −7.9 | 3.6 | −1.6 | −1.708 |
| | A2 | 3.1 | 3.8 | −4.5 | 3.5 | −7.3 | −5.2 | −2.3 | −3.1 | 2.7 | −2.6 | −7.7 | 3.6 | −1.6 | |
| | B1 | 2.3 | 3.6 | −4.2 | 3.9 | −7.8 | −5.6 | −2.6 | −3.6 | 2.8 | −3.5 | −7.7 | 3.4 | −1.9 | |
| 2041–2070 (“2050s”) | A1B | 4.2 | 4.7 | −2.9 | 4.9 | −6.6 | −4.6 | −1.6 | −1.8 | 4.3 | −1.9 | −6.7 | 4.8 | −0.6 | −0.980 |
| | A2 | 3.7 | 4.4 | −3.0 | 5.0 | −6.1 | −4.5 | −1.3 | −1.5 | 4.3 | −1.9 | −7.0 | 4.5 | −0.6 | |
| | B1 | 3.7 | 2.6 | −3.6 | 3.8 | −7.9 | −5.2 | −2.0 | −3.2 | 3.0 | −3.4 | −7.5 | 3.1 | −1.7 | |
| 2071–2000 (“2080s”) | A1B | 5.3 | 4.4 | −1.9 | 4.6 | −6.0 | −3.8 | −0.6 | −1.0 | 4.9 | −1.3 | −6.4 | 6.3 | 0.04 | 0.002 |
| | A2 | 6.7 | 6.8 | −1.2 | 6.1 | −5.0 | −3.1 | 0.5 | −0.1 | 6.1 | −0.6 | −6.0 | 6.8 | 1.1 | |
| | B1 | 3.9 | 4.5 | −2.7 | 4.5 | −6.9 | −5.2 | −2.0 | −2.5 | 3.5 | −3.2 | −7.0 | 4.2 | −1.1 | |
| Change in mean monthly air Temperature, $(\Delta T_{max} + \Delta T_{min})/2$ | | | | | | | | | | | | | | | |
| 2011–2040 (“2020s”) | A1b | 1.6 | 3.1 | 0.9 | 0.7 | 1.0 | 1.6 | 1.5 | 1.7 | 1.5 | 0.8 | 0.9 | 0.7 | 1.3 | 1.4 |
| | A2 | 2.0 | 2.8 | 0.6 | 0.4 | 1.2 | 1.7 | 1.8 | 1.8 | 1.1 | 0.9 | 1.0 | 0.8 | 1.3 | |
| | B1 | 1.7 | 3.6 | 1.5 | 1.0 | 1.1 | 1.3 | 1.6 | 1.3 | 1.2 | 1.2 | 1.1 | 1.1 | 1.5 | |
| 2041–2070 (“2050s”) | A1B | 3.1 | 3.6 | 2.2 | 1.2 | 1.7 | 2.0 | 2.5 | 2.7 | 2.2 | 1.7 | 2.0 | 1.8 | 2.2 | 2.1 |
| | A2 | 2.6 | 3.4 | 1.8 | 1.6 | 2.2 | 2.0 | 2.4 | 3.0 | 2.6 | 1.9 | 1.6 | 1.6 | 2.2 | |
| | B1 | 3.0 | 2.7 | 2.0 | 0.9 | 0.9 | 2.4 | 2.5 | 1.9 | 1.9 | 1.3 | 1.4 | 0.8 | 1.8 | |
| 2071–2000 (“2080s”) | A1B | 3.8 | 3.2 | 2.9 | 1.0 | 2.4 | 3.1 | 3.7 | 3.5 | 2.8 | 2.1 | 2.4 | 3.0 | 2.8 | 3.0 |
| | A2 | 5.2 | 5.3 | 3.3 | 2.2 | 3.4 | 3.7 | 4.5 | 4.6 | 4.0 | 2.7 | 2.8 | 3.6 | 3.8 | |
| | B1 | 3.8 | 4.3 | 3.0 | 1.6 | 2.1 | 2.1 | 2.4 | 2.7 | 1.8 | 1.3 | 1.8 | 1.8 | 2.4 | |





HESSD
10, 8503–8536, 2013



V. Mahat and A. Anderson

Title Page
Abstract | Introduction
Conclusions | References
Tables | Figures
◀| |▶
◀ ▶
Back | Close
Full Screen / Esc
Printer-friendly Version
Interactive Discussion

**Table 2.** Comparison of monthly statistics of daily precipitation, $T_{max}$ and $T_{min}$ observed at Coleman station during the period from 1965 to 1997 with synthetic data generated by LARS-WG. *P* values calculated by the *t* test and *F* test for the monthly means and variances are shown. A probability of 0.05 or lower indicates a departure from the observations that is significant at the 5 % level.

| | Jan | Feb | Mar | Apr | May | Jun | Jul | Aug | Sep | Oct | Nov | Dec |
|---|---|---|---|---|---|---|---|---|---|---|---|---|
| Precipitation | | | | | | | | | | | | |
| Observed mean | 45.10 | 39.13 | 34.98 | 39.03 | 63.24 | 67.58 | 52.56 | 50.98 | 44.42 | 38.19 | 48.70 | 45.91 |
| Observed standard deviation | 31.80 | 31.59 | 21.59 | 17.63 | 29.39 | 26.19 | 40.22 | 39.99 | 26.67 | 24.34 | 33.15 | 30.23 |
| Generated mean | 41.36 | 33.85 | 35.42 | 39.34 | 57.96 | 71.61 | 60.82 | 52.11 | 41.01 | 39.62 | 56.99 | 38.60 |
| Generated standard deviation | 21.67 | 17.00 | 20.24 | 17.64 | 25.49 | 25.81 | 23.65 | 20.02 | 22.19 | 21.19 | 32.38 | 22.44 |
| *P* values for *T* test | 0.583 | 0.406 | 0.933 | 0.943 | 0.442 | 0.535 | 0.319 | 0.887 | 0.577 | 0.803 | 0.315 | 0.276 |
| *P* values for *F* test | 0.036 | 0.001 | 0.720 | 0.995 | 0.431 | 0.936 | 0.03 | 0.03 | 0.309 | 0.445 | 0.896 | 0.102 |
| $T_{min}$ | | | | | | | | | | | | |
| Observed mean | −13.05 | −10.09 | −6.87 | −2.63 | 1.35 | 4.95 | 6.61 | 5.86 | 2.46 | −0.46 | −6.39 | −11.15 |
| Observed standard deviation | 4.76 | 4.06 | 2.93 | 1.69 | 0.95 | 1.16 | 1.02 | 1.20 | 1.38 | 1.58 | 3.16 | 4.32 |
| Generated mean | −10.41 | −9.10 | −5.21 | −2.51 | 1.32 | 4.93 | 6.15 | 5.33 | 2.07 | −1.13 | −5.30 | −9.67 |
| Generated standard deviation | 1.82 | 1.72 | 1.32 | 0.83 | 0.65 | 0.71 | 0.49 | 0.63 | 0.97 | 1.21 | 1.44 | 1.73 |
| *P* values for *T* test | 0.005 | 0.208 | 0.005 | 0.734 | 0.914 | 0.944 | 0.024 | 0.031 | 0.188 | 0.062 | 0.080 | 0.078 |
| $T_{max}$ | | | | | | | | | | | | |
| Observed mean | −3.51 | −0.02 | 3.55 | 8.91 | 14.22 | 18.38 | 22.37 | 22.36 | 16.90 | 10.41 | 1.66 | −2.83 |
| Observed standard deviation | 4.07 | 3.14 | 2.85 | 2.21 | 1.85 | 1.84 | 2.14 | 2.55 | 3.43 | 2.23 | 2.91 | 3.34 |
| Generated mean | −1.25 | 0.64 | 4.64 | 9.21 | 14.24 | 18.30 | 22.12 | 21.84 | 16.85 | 9.66 | 2.33 | −1.86 |
| Generated standard deviation | 1.38 | 1.13 | 0.83 | 1.09 | 1.22 | 0.93 | 1.08 | 1.04 | 1.38 | 1.30 | 1.10 | 1.19 |
| *P* values for *T* test | 0.006 | 0.263 | 0.052 | 0.499 | 0.957 | 0.826 | 0.558 | 0.282 | 0.935 | 0.106 | 0.227 | 0.128 |

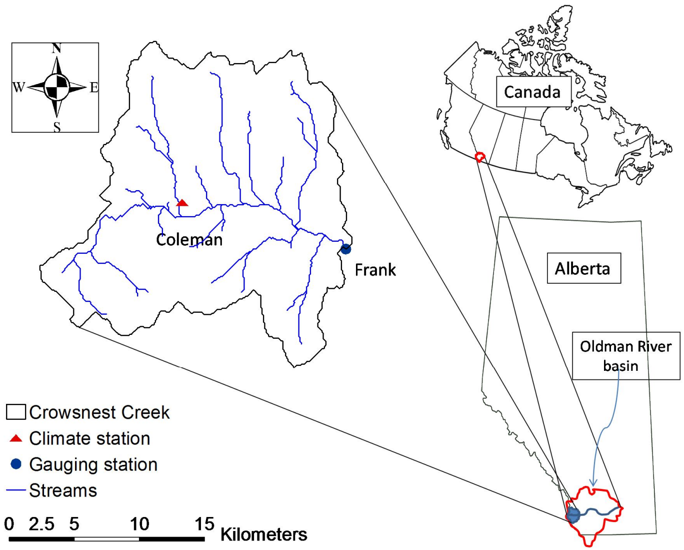


**Fig. 1.** Crowsnest Creek watershed with climate station, Coleman and gauging station, Crowsnest at Frank.





HESSD
10, 8503–8536, 2013



V. Mahat and A. Anderson

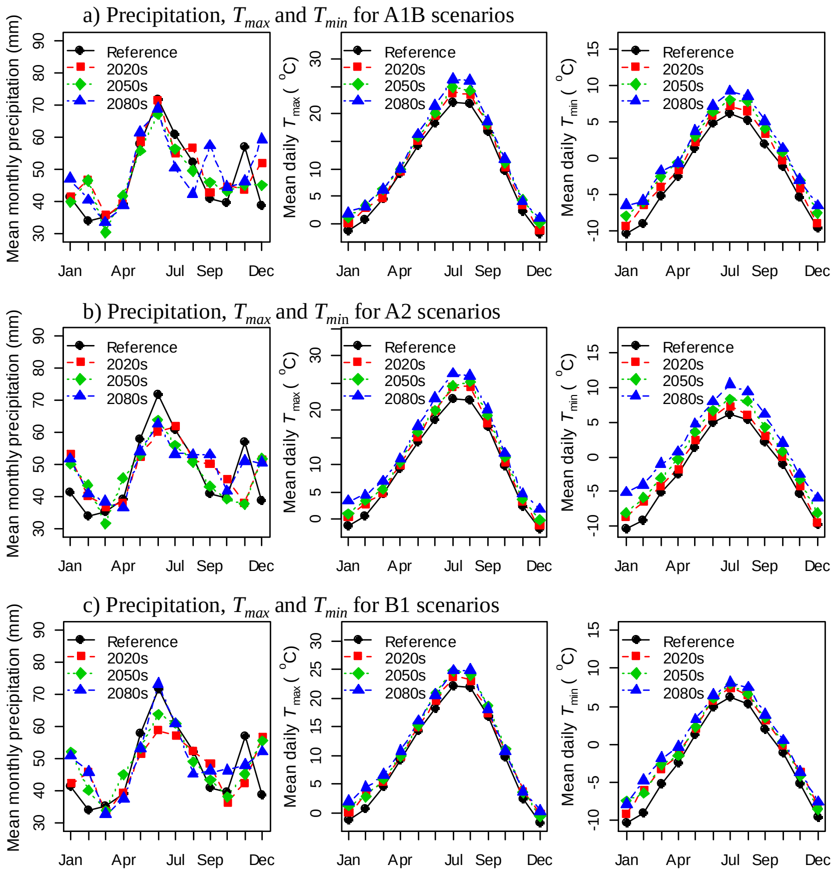


**Fig. 2.** Reference (observed) period daily climates aggregated to monthly scale and nine sets of future monthly climate means (precipitation, $T_{max}$ and $T_{min}$) estimated for climate station, Coleman.

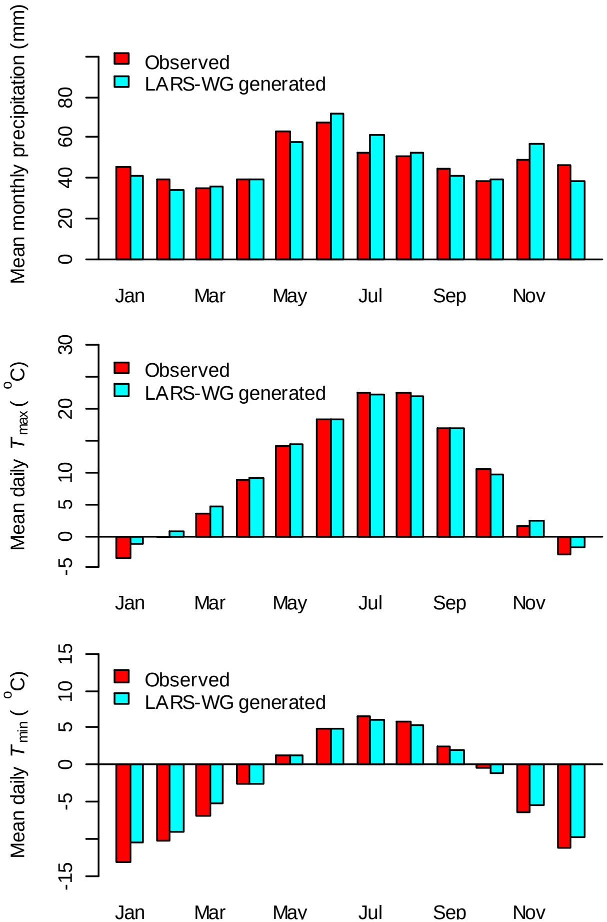


**Fig. 3.** Observed and LARS-WG generated monthly values of precipitation, $T_{max}$ and $T_{min}$.





HESSD
10, 8503–8536, 2013

Impacts of climate and forest changes on streamflow

V. Mahat and A. Anderson

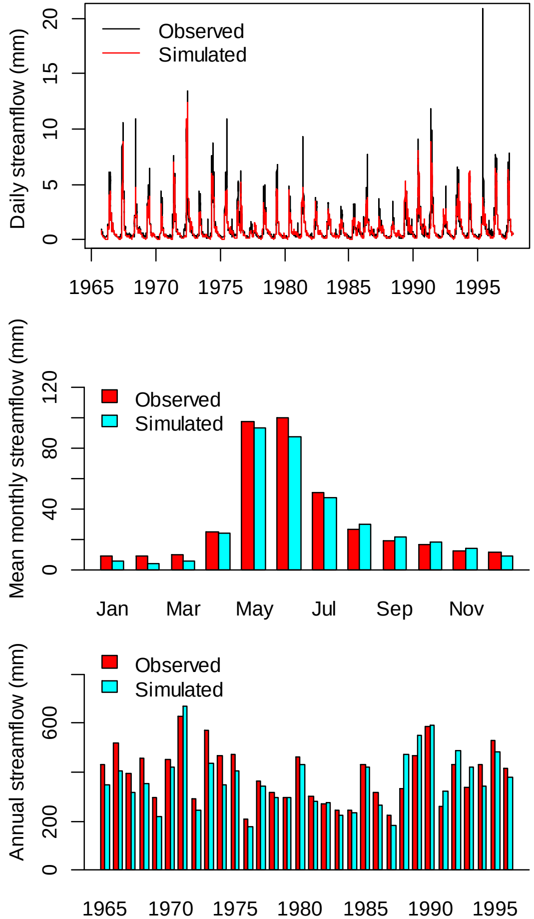


**Fig. 4.** Observed and HBV-EC simulated daily, monthly and annual streamflows during the calibration period from 1965 to 1997. HBV-EC is driven by the daily climates observed at Coleman station.





HESSD
10, 8503–8536, 2013

Impacts of climate and forest changes on streamflow

V. Mahat and A. Anderson

Title Page
Abstract Introduction
Conclusions References
Tables Figures
◀| |▶
◀ ▶
Back Close
Full Screen / Esc
Printer-friendly Version
Interactive Discussion

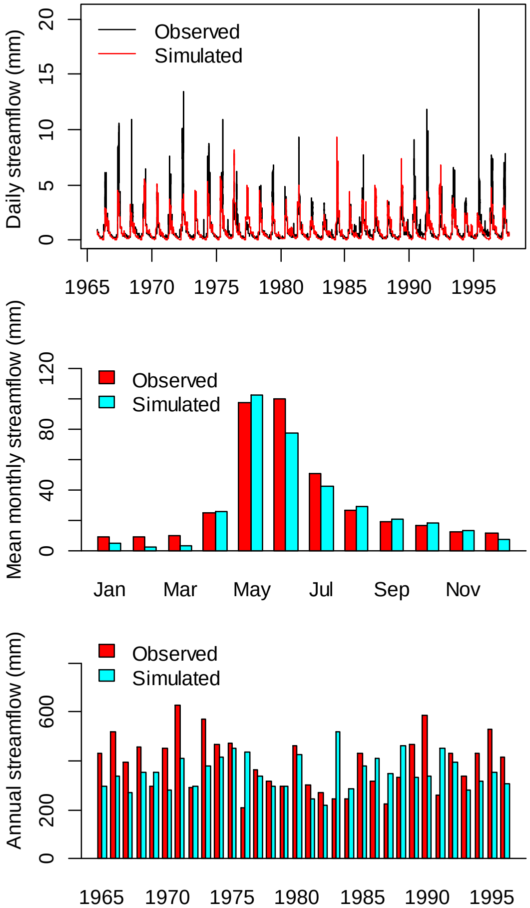


**Fig. 5.** Same as Fig. 4, but in this case HBV-EC is driven by the LARS-WG generated daily climates.





HESSD
10, 8503–8536, 2013

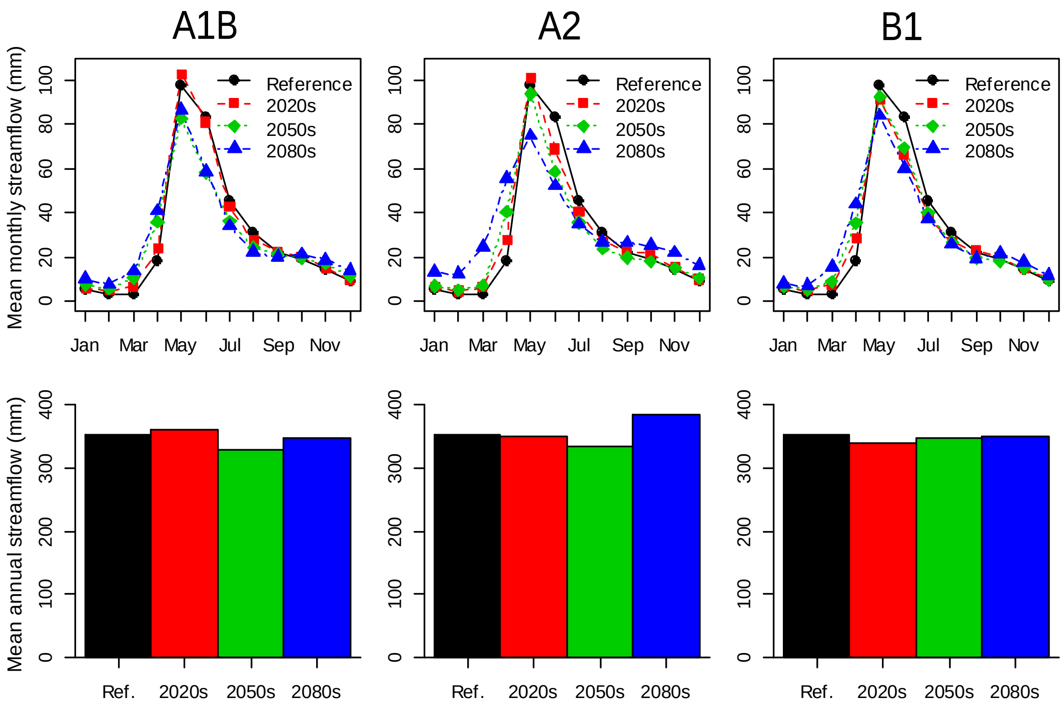


**Fig. 6.** HBV-EC simulated mean monthly and mean annual streamflows for the reference and nine future periods (for three different scenarios: A1B, A2 and B1 and for three different time periods: 2020s, 2050s and 2080s) at the watershed outlet at Crowsnest at Frank.






HESSD
10, 8503–8536, 2013


Impacts of climate and forest changes on streamflow


V. Mahat and A. Anderson

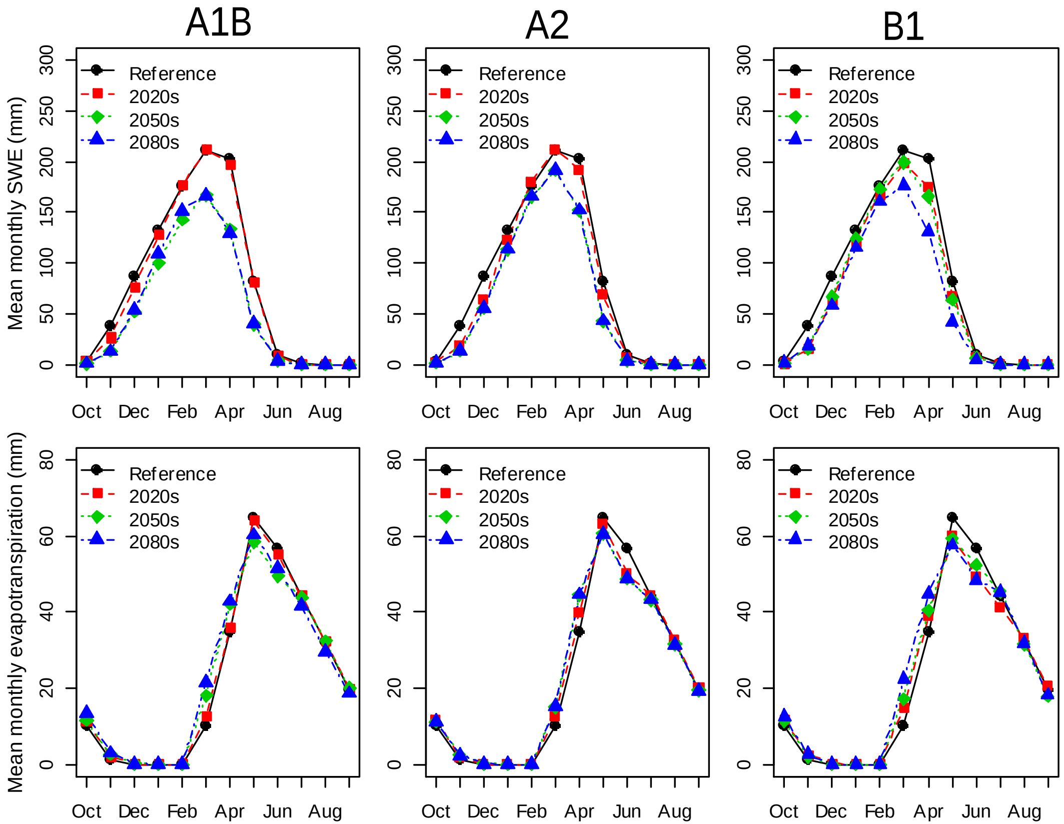


**Fig. 7.** HBV-EC simulated watershed averaged mean monthly snow water equivalent (SWE) and mean monthly evapotranspiration for the reference and future periods.





HESSD
10, 8503–8536, 2013

Impacts of climate and forest changes on streamflow

V. Mahat and A. Anderson

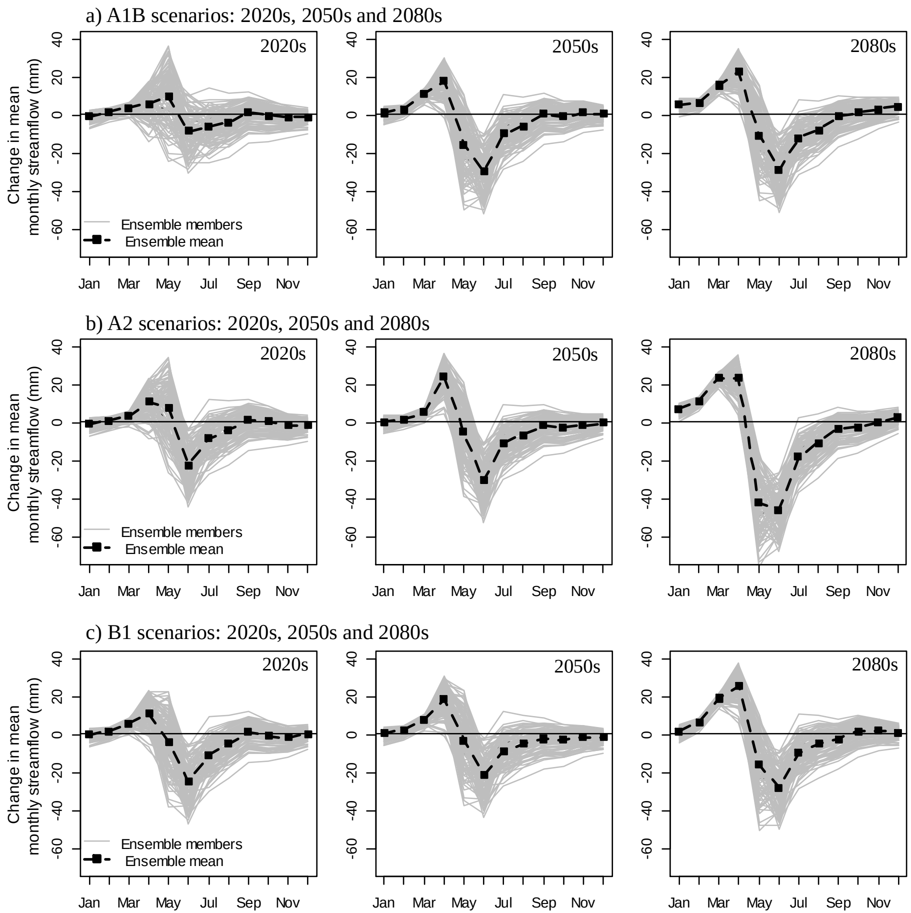


**Fig. 8.** Ensemble of relative changes in mean monthly streamflows in different future periods compared to reference period streamflow; and mean of the ensemble.

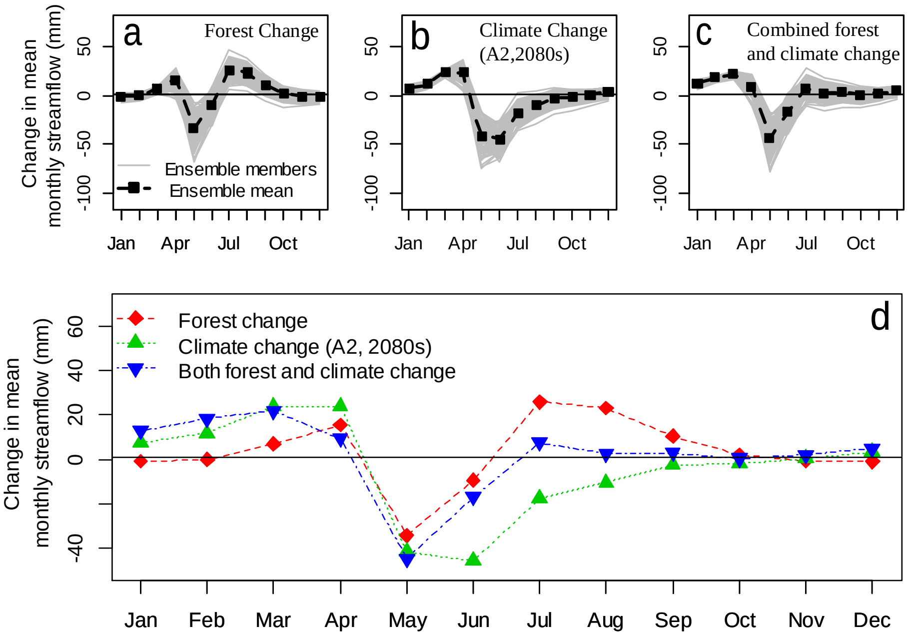


**Fig. 9.** Ensemble and mean values of relative changes in mean monthly streamflows: **(a)** due to forest removal **(b)** due to climate change in 2080s in A2 scenario and **(c)** due to combined forest removal and climate change in 2080s in A2 scenario. **(d)** shows the ensemble mean to compare the relative changes in mean monthly streamflows due to forest removal, due to climate change in 2080s in A2 scenario and due to combined forest removal and climate change in 2080s in A2 scenario.





HESSD
10, 8503–8536, 2013

Impacts of climate and forest changes on streamflow

V. Mahat and
A. Anderson

Title Page
Abstract Introduction
Conclusions References
Tables Figures
◀ ▶
Back Close
Full Screen / Esc
Printer-friendly Version
Interactive Discussion